Influence of Ion Pairing on the UV-Spectral Behavior of KI Dissolved in Supercritical NH_3: From Vapor Phase to Condensed Liquid

Germán Sciaini,[†] Ernesto Marceca,[†] and Roberto Fernández-Prini*[,†,‡]

INQUIMAE-DQIAQF, Facultad Cs. Exactas y Naturales, University of Buenos Aires, Ciudad Universitaria, Pabellón II, Buenos Aires, Argentina, and Unidad Actividad Química, Comisión Nacional Energía Atómica, Av. Libertador 8250, Buenos Aries, Argentina

Received: June 24, 2005; In Final Form: August 12, 2005

The UV-spectroscopic behavior of KI dissolved in supercritical ammonia enabled us to identify two species that contribute to the optical absorption depending on the fluid density ρ_1 and the temperature *T*. At low ρ_1 and high *T*, contact ion pairs (CIPs) prevail, while at high density of ammonia, solvent separated ion pairs (SSIPs) and free iodide ions dominate the optical absorption of the solute. The features of the electron excitation process depend on the state of the K^+I^- species present. Starting with isolated KI in the vapor, where the process is an interionic charge transfer, when the CIP becomes solvated the UV absorption shifts strongly to the blue. As ρ_1 increases, the amounts of SSIP and of free iodide increase progressively and their electronic excited states become those characteristic of the charge-transfer-to-solvent process. This study suggests there is a strong influence of the cation on the electronic transition of dissolved iodide when it is forming CIPs. Moreover, the fact that K^+-NH_3 interaction is much larger than that of I^--NH_3 suggests that the electronic photoinduced excited state of CIPs is similar to the ground state observed for alkali metals in NH_3 clusters.

Introduction

Isolated halogen anions do not have bound electronic excited states below the photodetachment threshold, and electrons reach the continuum when photoexcited.[1] On the other hand, if anions are surrounded by polar solvent molecules, then photoexcitation promotes an electron to a somewhat asymmetric diffuse state around the halogen atom, a level analogous to a Rydberg state,[2] which is bound by the force field of the surrounding solvent molecules. This process epitomizes the well-known charge-transfer-to-solvent (CTTS) excitation and is the reason CTTS bands have been considered a means of inquiring into the nature of the solvation of anions.

The CTTS bands of anions have been studied for about 50 years; the results of the work carried out in a variety of liquid solvents were covered in detail by Blandamer and Fox in 1970.[1] However, in the last 15 years interest in the CTTS bands has been renewed with the publication of experimental, theoretical, and simulation studies,[3] in particular studying the analogue to the CTTS process in solvent clusters with anions or, in a few cases, with ion pairs.[4] This is so because in clusters electronic excitation of anions occurs in partially confined systems which have a limited capacity for the manifestation of long-range polarization effects. Moreover, it has recently been stressed that the study of simple processes, such as CTTS, is important in order to gain a clear insight of the general role of solvation[5] (a complex phenomenon in itself) on chemical processes and also because it is considered to be a step in the process of electron excitation leading ultimately to its detachment to the solvent and to other photo processes.

It is known[4] that the electronic excitation of the ($X^1\Sigma_0^+$) ground state in the isolated KI (vapor phase) leads to an interionic charge transfer from the iodide ion to the cation and the electron is promoted to a covalent ($\Omega = 0^+$) excited state. However, when KI is dissolved in a polar liquid solvent, it will dissociate and the I^- electronic excitation will lead to CTTS states. It has been argued[1,6] that CTTS bands are not bedevilled by the contributions of different species, nevertheless it has been noted that for low dielectric constant solvents, where electrolytes are mainly in the form of ion pairs, the position of the CTTS band shifted when an alkali metal cation was exchanged by an alkyl substituted ammonium ion.[7] Thus, the use of the electronic transitions of alkali metal halides as a means of describing the solvent environment should take into account the effect of ion pairing upon the spectral behavior. Through the use of a supercritical polar solvent, it is possible to change widely the medium polarity varying solvent density so that the medium may change continuously from a dense polar liquid to a low-density vapor. Ion pairs will be increasingly formed as the fluid density decreases, and it is interesting to inquire about the evolution of the spectral behavior between the two extremes.

Our objective in the present study was to analyze by UV spectroscopy the effect that different species in solutions of KI in a polar solvent have on electronic excitation, that is, starting with the isolated (K^+I^-) pair, going to contact (CIP) and solvent separated (SSIP) ion pairs, and finally to free ions in solution. We have chosen ammonia as the solvent medium under sub- and supercritical conditions; changes in solvent density (ρ_1) and/or temperature (*T*) will cause changes in its dielectric constant and hence in the species prevailing in the solutions. Buback and Harder have measured the dielectric constant of NH_3 over a wide range of (ρ_1, *T*),[8] so this important information is already available. Moreover, the use of a polar supercritical solvent should allow us to establish how the electronic spectra of alkali metal iodides are affected by changes in the concentration of the species present in the solutions, as well as their dependence

* To whom correspondence should be addressed. E-mail: rfprini@cnea.gov.ar.
[†] University of Buenos Aires.
[‡] Unidad Actividad Química.

10.1021/jp053446g CCC: $30.25
Published on Web 09/17/2005

on ρ_1 and T. Thus, ammonia can be considered a good solvent to test many of the dominant ideas in the field.

The study of the CTTS process is usually carried out for one of the following reasons: (i) because it reflects the solvent environment surrounding the anion and (ii) because it is an important step in the photophysical process that leads to electron detachment in a solvent. In the present work, we have been able to identify different UV-absorption bands due to the various species present in the solutions and establish the influence of the cation. Hence, the first reason for studying CTTS should be revised to take into account the effect of ion pairing upon the spectral behavior of KI.

Experimental Section

Details of the experimental setup and measuring equipment have been given in the first report of this research[9] where solubility data for alkali metal iodides dissolved in NH_3 as function of the solvent's density have been given; we only give here a brief account. For the present part of the study, we employed a high-pressure spectrophotometric cell having an optical path of 2.04 cm and sapphire windows; the cell was electrically heated and the temperature fixed with a proportional−integral−differential controlling system. The cell had a magnetic stirrer that was operated from the outside. The ancillary equipment necessary to prepare the solutions at variable solvent densities consisted of a manual pressure pump, two pressure transducers, and two Pt resistances as thermometers. NH_3 was AGA 99.99% and crystalline pa. KI was used without further purification. We introduced the cell into a Shimadzu spectrophotometer UV-3101PC and recorded the spectra between 220 and 350 nm with a wavelength resolution of 1 nm, that is, between 5.64 and 3.54 eV with a resolution of 0.02 eV.

The main spectroscopic determinations were performed for KI solutions at 418 K where the density was systematically changed. Since the critical temperature of NH_3 is 405.4 K,[10] the temperature of our study was sufficiently high to minimize the contribution of any near-critical effect[11] upon the measurements. To calculate the molar absorptivity of the optically active species, we prepared subsaturated KI solutions in supercritical NH_3 (SCA). This operation was carried out very carefully so that the actual value of the concentration of KI could be established with precision.[9] The UV-absorption spectra at four fluid densities were recorded and used to determine the molar absorptivities of the species contributing to them.

We also recorded the spectra for KI solutions having approximate concentrations of 5×10^{-5} mol dm^{-3} at 418 K and at several values of ρ_1. These measurements were employed to obtain the ρ_1 dependence of the transition energy at the band's maximum (E_{max}), hence it was not necessary to know with precision the value of KI concentration. Finally, we measured the UV absorption of KI solutions in liquid NH_3 at different temperatures and at the saturation pressure; this information together with that already available in the literature allowed us to confirm the existence of two UV-absorbing species in our solutions. The density of SCA was calculated from the experimental pressure and temperature of the solutions using the equation of state proposed by Tillner-Roth et al.[10]

Molecular Dynamics Simulations and ab Initio Calculations

Constant−NVT molecular dynamics (MD) runs with periodic boundary conditions (applying the particle mesh Ewald summation method) were carried out using the AMBER8 package.[12] For the intermolecular interaction of solvent molecules, the rigid model for the ammonia molecule proposed by Impey and Klein[13] was used; in this model, NH_3 has partial charges in four sites and a Lennard-Jones core. The potassium and the iodide ions interacted with other particles through their charges and Lennard-Jones terms as given for the i−j interactions in Table 1.

TABLE 1: Lennard-Jones Interaction between NH_3 Sites and Ions According to the Equation: $V_{ij}(LJ) = A_{ij}/r^{12} - B_{ij}/r^6$

i−j	A_{ij}/(eV·nm^{12}/mol)	B_{ij}/(eV·nm^6/mol)
K−N	3.0345×10^{-6}	1.1705×10^{-3}
I−N	1.0621×10^{-7}	2.8178×10^{-4}
K−I	3.6848×10^{-7}	2.2976×10^{-4}
N−N[a]	1.1505×10^{-7}	7.4471×10^{-5}

[a] Reference 13.

TABLE 2: Values of the Energy Minimum and Equilibrium Distance between Sites and Ions Obtained by Energy Minimization

	values obtained for each i−j pair interaction by energy minimization		values from experiment or ab initio calculations	
V_{i-j}	E_{min}/eV	r_{eq}/nm	E_{min}/eV	r_{eq}/nm
$V_{K^+-NH_3}$	0.871	0.283	0.871[14]	0.283 (pw)[a]
$V_{I^--NH_3}$	0.316	0.400	0.320[14]	0.398 (pw)[a]
$V_{K^+-I^-}$	4.44	0.307	4.45[15]	0.305−0.310[16]

[a] pw: present work (ab initio calculations).

The values given in Table 1 for the Lennard-Jones coefficients of all interacting pairs of particles were fixed such that the minimum energy of each pair at 0 K calculated with AMBER8 gave results close to the experimental[14] or ab initio values calculated in the present work for K^+-NH_3, I^--NH_3, and K^+-I^- interactions. The details are reported in Table 2.

The MD runs were made for one K^+ and one I^- in 215 and 1000 ammonia molecules to establish the influence of box size upon the distribution of the K^+-I^- interionic distance; the evolution of the simulated system was followed for 200 or 400 ps using a time step of 0.4 fs. Also, systems consisting of I^- in NH_3 were employed to simulate the behavior of dissolved free iodide. Runs for several values of ρ_1 and T were carried out to gain a qualitative insight about speciation in the solutions.

The dipole moment of the rigid NH_3 molecule is 5.00×10^{-30} C m (1.50 D), which is slightly larger than the experimental value (1.48 D).[8] This model Hamiltonian for NH_3 yields an appreciably smaller dielectric constant ϵ_D for liquid ammonia at 294 K;[17] however it gives a very reasonable account of the thermodynamic and structural properties of liquid ammonia[13,18] and has been used previously to model SCA.[19]

The Gaussian98 package[20] was employed to calculate the electronic excitation energies. The calculations were performed according to a computational strategy which combines a high-level quantum electronic structure method with an efficient MD trajectory-sampling technique. This approach proposed by Bradforth and Jungwirth[21] was successfully applied to study the CTTS states of iodide anions dissolved in bulk water. The electronic transition energies were taken as the difference between the lowest triplet and singlet states employing the Möller−Plesset second-order perturbation theory (MP2). We used quantum solutes with a very diffuse basis set and the same rigid point charge model for ammonia molecules used in MD simulations. For the iodine atom, we have employed LANL2DZ diffused basis functions with a pseudopotential core. This basis set has been augmented by a very diffuse s set with eight exponents forming a geometric series with a factor of 2 and lowest exponent of 1.406×10^{-3} plus a p set with an exponent of 0.500 and six exponents forming a geometric series with a

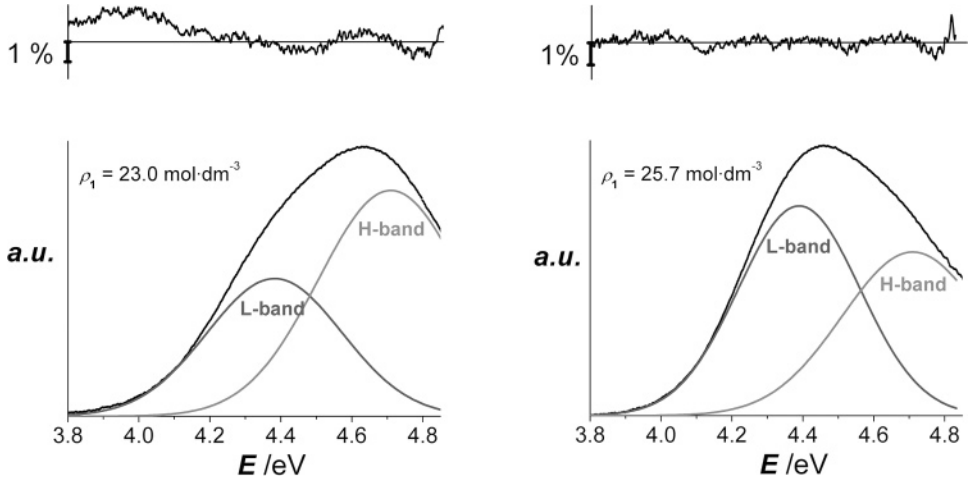

Figure 1. Spectra of KI at 418 K and two different ammonia densities (ρ_1) fitted by two Gaussians. H-bands correspond to the CIP, and L-bands, labeled as I^- in the text, correspond to free iodide and SSIP. The upper panels show the percent residuals of the fitted curves. Note that $Q = c_{I^-}/c_{CIP}$ increases with ρ_1; a.u. are arbitrary units of optical absorption.

factor of 2 and lowest exponent of 4.688×10^{-4} plus a d basis with an exponent of 0.100. For the potassium atom, we have employed the diffused and polarizable 6-31++G* basis set.

The E_{max} values for the CIP and free I^- at different (ρ_1, T) conditions were obtained by averaging the calculated electronic transition energy for about 100 randomly selected snapshots along the MD run. Further details for the validation of the Bradforth and Jungwirth strategy when applied to our systems will be given in a forthcoming article. In the present work, the calculated E_{max} values are given only with the purpose of confirming the speciation found by careful analysis of the experimental spectra.

Results

In our previous work on alkali metal iodides in SCA,[9] we reported that E_{max} values for the NaI and CsI UV bands in solutions at low solvent density were at 4.76 and 4.67 eV, respectively. These are different from the intermediate value $E_{max} = 4.71$ eV observed for KI, hence the maxima are displaced to the red when the size of the cation increases. This behavior is expected if the ions are essentially in the form of CIPs;[1] in that study, carried out at low NH_3 densities and a temperature of 418 K, the CIP species prevailed in the iodide solutions. In the present work, we have studied the UV spectrum of KI dissolved in SCA at higher ρ_1 values. The energy of the UV band maximum at 418 K showed almost no shift with ammonia density until ρ_1 was above 16 mol·dm^{-3}. At higher densities, the maximum of the absorption band shifted slightly to the red as fluid density increased, and at the same time, the band showed some asymmetry. These facts could only be accounted for if two contributions to the overall UV band were assumed to exist. This is illustrated in Figure 1 where the spectra for KI in ammonia at densities of 23.0 and 25.7 mol·dm^{-3} at 418 K are shown. The experimental bands were decomposed into two Gaussian curves after subtracting the optical absorption baselines, no parameters were fixed during the fitting procedure. The upper panels of Figure 1 show the percent residuals of the fitted curves evidencing a small fitting error.

In the figure, the two contributions to the overall broad UV-absorption band are shown; the height and area of the contribution having lower E_{max} (L-band) values increase with ρ_1 while they decrease for the other component band. The higher energy band (H-band) was assigned to the CIP since it coincides with that observed at low ρ_1 values. The L-band was assigned to free iodide or SSIP (vide infra the discussion about the contribution of these two species to optical absorption).

TABLE 3: E_{Max} for the Overall Band and the L-Band at Saturation Pressure (except *b*)

T/K	L-band E_{max}/eV	overall E_{max}/eV	ρ_1/mol·dm^{-3}	ref
195.2		5.02		11
223.2		4.97	41.2	11
293.2		4.69	35.8	12
300.5	4.66	4.67	35.2	pw[a]
301.8		4.67	35.1	12
310.7		4.64	34.3	12
319.7		4.62	33.4	12
327.2		4.60	32.6	12
348.5	4.52	4.54	30.3	pw
366.8	4.48	4.51	27.8	pw
380.1	4.45	4.50	25.6	pw
402.7	4.39	4.55	23.9	pw[b]
418.2	4.35	4.64	23.0	pw[b]

[a] pw: present work. [b] Points measured at $\rho_1 \approx 23.5$ mol·dm^{-3} (cf. text).

For $\rho_1 \leq 12$ mol·dm^{-3} only the contribution of the H-band could be determined because the contribution of the other species to the overall optical absorbance was too small and its parameters could not be determined with enough precision.

An important evidence for the presence of more than one species in ammonia was obtained from the analysis of data in liquid ammonia at saturation pressure measured by us and by other authors. Nelson et al.[22] and Shapira and Treinin[23] studied the UV absorption of KI dissolved in liquid ammonia (Table 3); the maximum wavelength of the band they reported at different temperatures and saturation pressures was assumed to be due to the free I^- ion. This seems to be a reasonable assumption, taking into account our experimental results and, as shown below, the fact that the CTTS processes of solvent separated ion pairs and the free iodide ion are very similar. We have also recorded the UV spectra of KI in liquid NH_3 at saturation pressure and higher temperatures; the values of E_{max} for the overall band are also reported in Table 3. The last two points, liquid at 402.7 K and SCA at 418.2 K, do not correspond to the coexistence curve because the solvent was too compressible at those temperatures; their spectra were determined at ρ_1 around 23.5 mol·dm^{-3}.

The values of E_{max} are plotted in Figure 2; at low temperatures, the energy of the overall band decreases almost linearly with increasing temperature, then it goes through a minimum

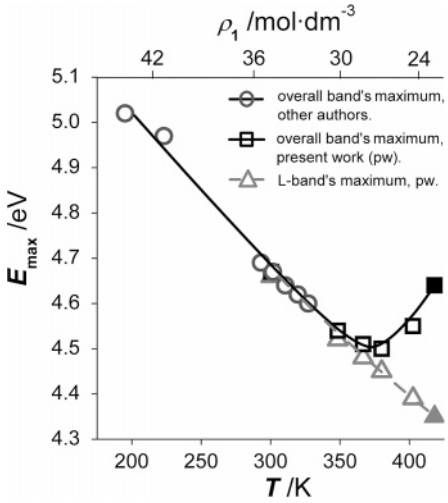

Figure 2. Temperature and density dependence of the absorption maximum along the liquid−vapor coexistence curve (except the last two points, cf. text) for the overall band (without decomposition in two bands) and the contribution of the L-band (I^-). Solid symbols correspond to a supercritical state.

at ca. 380 K after which it increases sharply with T. We attribute the change of sign in the slope of the curve to an increase in the fraction of iodide ion that is in the form of the CIP (greater at higher temperature and lower ρ_1 values) compared with the fraction of free anion or solvent separated ion pairs. It is obvious that the whole set of data in Table 3, those in liquid ammonia obtained at low temperature and those corresponding to the I^- species at higher temperature, are very consistent confirming that they refer to the same species, that is, the iodide ion that is not forming contact ion pairs. At low temperatures, E_{max} for I^- is the same as the overall E_{max}, but as temperature increases (or solvent density decreases) the two become very different due to the appearance of CIPs.

The stoichiometric (total) salt concentration, c_t, is related to the optical absorption due to both bands A_{CIP} and A_{I^-} by

$$c_t = \frac{A_{I^-}}{\epsilon_{I^-} l} + \frac{A_{CIP}}{\epsilon_{CIP} l} \tag{1}$$

where I^- represents all species not forming CIPs, l is the optical path of the cell, and ϵ_S is the molar absorptivity of species S. Equation 1 may be written as

$$\frac{A_{I^-}}{A_{CIP}} = \frac{c_t \epsilon_{I^-} l}{A_{CIP}} - \frac{\epsilon_{I^-}}{\epsilon_{CIP}} \tag{2a}$$

$$\frac{A_{CIP}}{A_{I^-}} = \frac{c_t \epsilon_{CIP} l}{A_{I^-}} - \frac{\epsilon_{CIP}}{\epsilon_{I^-}} \tag{2b}$$

To calculate the molar absorptivity of the two bands contributing to the observed total UV absorption, a solution of KI having a carefully determined concentration of 3.37×10^{-5} mol·dm^{-3} was prepared and its spectrum was recorded at 418 K (cf. Table 4) and different fluid densities.[9]

Only four data points of this run could be used because, as mentioned above, for those having $\rho_1 \leq 12$ mol·dm^{-3}, one of the species contributed very little to the spectra. Under the conditions of the four data points which were used, the concentration of both species made appreciable contributions to the total optical absorption. With the values of the UV absorption due to each species, (A_{I^-}/A_{CIP}) and (A_{CIP}/A_{I^-}) were calculated and plotted against $(A_{CIP})^{-1}$ and $(A_{I^-})^{-1}$, respectively;

TABLE 4: Component Bands of KI UV Absorption in Supercritical NH_3 at 418.2 K and Concentration of 3.37 × 10^{-5} mol·dm^{-3} Used To Determine the Molar Absorptivity of Each Band[a]

	CIP (H-band)		I^- (L-band)	
ρ_1/mol·dm^{-3}	A_{CIP}	E_{max}/eV	A_{I^-}	E_{max}/eV
16.1	0.464	4.70	0.056	4.19
18.6	0.438	4.71	0.073	4.25
21.3	0.408	4.71	0.132	4.32
23.0	0.380	4.71	0.179	4.35

[a] Values of A_B correspond to the optical absorption at the maximum of each B-band.

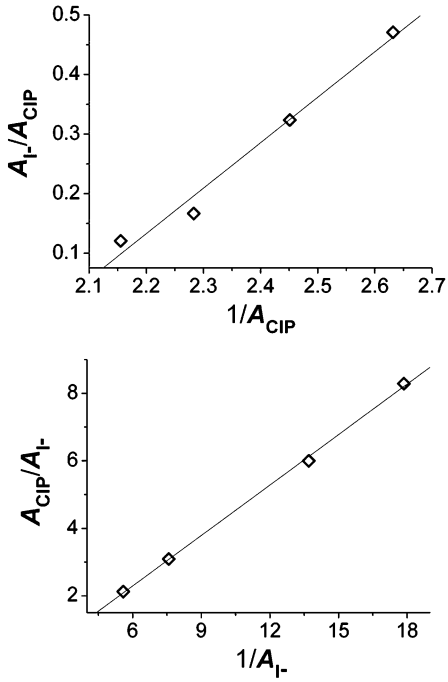

Figure 3. Linear plots used to calculate the molar absorptivities for the L- and H-bands, I^- and CIP, respectively, from the slopes according to eq 2.

their slopes yielded $\epsilon_{CIP} = 710 \pm 80$ m^2·mol^{-1} and $\epsilon_{I^-} = 1110 \pm 140$ m^2·mol^{-1} for the molar absorptivities of the two contributing bands. Figure 3 shows the straight lines from which the molar absorptivities were calculated using eq 2. It should be noted that ϵ_{CIP} is slightly bigger than the value we had reported[8] because the contribution of the free I^- ion was previously neglected since the values of ρ_1 were quite low; however, this small contribution is responsible for this difference.

The values of the ratio $Q = (c_{I^-}/c_{CIP})$ were then calculated using A_S and ϵ_S for species S as with

$$Q = \frac{c_{I^-}}{c_{CIP}} = \frac{\epsilon_{CIP} A_{I^-}}{\epsilon_{I^-} A_{CIP}} \tag{3}$$

It should be remarked that Q calculated with eq 3 is a direct result of the experimental determination of the contributions of the two bands to the overall UV absorption. Figure 4 shows the ratio Q plotted against the fluid density for two different KI total concentrations. Both sets of data points show that c_{I^-} is very small until ρ_1 reaches 12 mol·dm^{-3}; the value of Q increases sharply above 22 mol·dm^{-3}.

It should be remembered that our MD results cannot be used to characterize quantitatively the association process because of the low dielectric constant given by the effective Hamiltonian we used for NH_3 which, however, is known to be adequate to

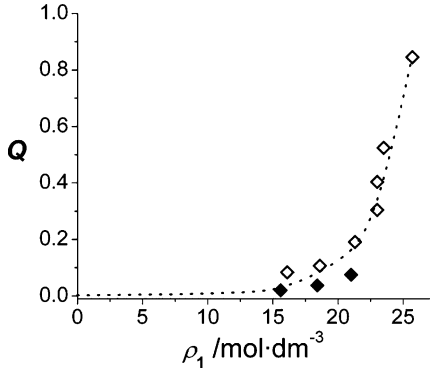

Figure 4. Plot of $Q = c_{I^-}/c_{CIP}$ as function of solvent density. Open and solid symbols correspond to c_t around 3.8×10^{-5} and 13.0×10^{-5} mol·dm^{-3}, respectively. Note that dissociation of the CIP starts becoming significant at $\rho_1 \approx 22$ mol·dm^{-3}.

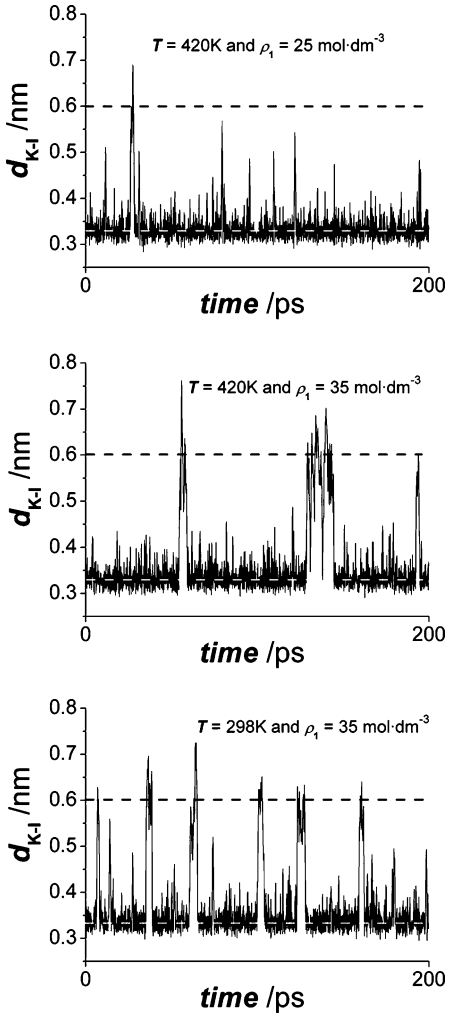

Figure 5. K^+-I^- distance (d_{K-I}) for a simulation run of 200 ps. The dashed lines at 0.60 and 0.33 nm represent the typical values of d_{K-I} for the SSIP and CIP, respectively.

describe the thermodynamic and structural properties of fluid ammonia. Figure 5 shows the value of the K−I distance for a 200 ps simulation run at 420 K and two densities; it is observed that the frequency of events leading to SSIP formation increases as ρ_1 goes from 25 mol·dm^{-3} (close to the experimental value of 22 mol·dm^{-3} where Q varies sharply) to 35 mol·dm^{-3}. The run for 298 K and 35 mol·dm^{-3} (simulation box of 2.7 nm) also illustrated in Figure 5 shows the increase in the number of SSIP configurations as temperature was reduced.

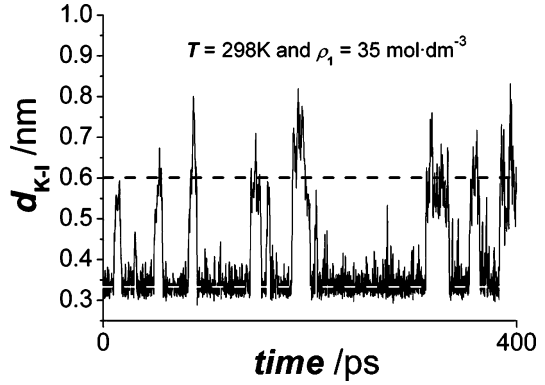

Figure 6. K^+-I^- distance for a simulation run of 400 ps. The dashed lines at 0.60 and 0.33 nm represent the typical values of d_{K-I} for the SSIP and CIP, respectively. The simulation box had a dimension of 3.60 nm in this case.

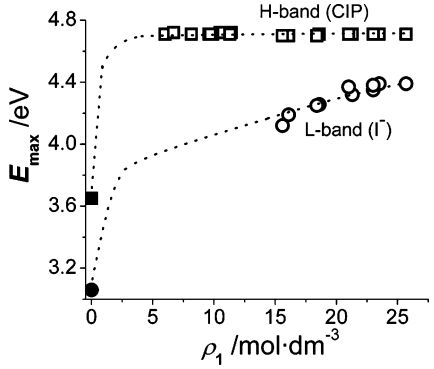

Figure 7. Experimental dependence of the H-band (□) and L-band (○) E_{max} with solvent density at 418 K. The H-band corresponds to CIP and the L-band to I^- not forming contact ion pairs. Dotted lines represent the expected behavior. Solid symbols are the values at zero ρ_1, that is, for isolated I^- (ref 24) and isolated K^+I^- (ref 25), respectively.

Figure 6 shows the values of the K^+-I^- distance for a 400 ps simulation run in liquid NH_3 at 298 K and 35 mol·dm^{-3} for a larger simulation box of 3.6 nm; the pattern of CIP and SSIP is similar to that in Figure 5, but no events corresponding to free I^- were observed, probably due to the low dielectric constant of the model NH_3. It may be noted that the interionic distance in CIPs corresponds to an average distance of 0.33 nm, while the average interionic distance for SSIPs is observed at around 0.6 nm independently of the simulation box size.

Figure 7 shows the experimental dependence of E_{max} on fluid density at 418 K for each band. The H-band corresponding to the CIP is almost unaffected by changes in ρ_1 over a wide range of densities, while the L-band corresponding to the free I^- and/or SSIP shifts to the blue as fluid density increases.

Figure 8 shows the fluid density dependence of E_{max} at 420 K calculated for the CIP and the free iodide ion. As described above, the values of E_{max} were obtained using the Gaussian98 package and averaging the electronic transition energy over 100 randomly selected snapshots along the MD runs; for CIPs, we only employed snapshots for which the K^+-I^- distance was smaller than 0.40 nm. The comparison between experimental (Figure 7) and calculated (Figure 8) E_{max} is considered to support our assignment of the bands; their somewhat different ρ_1 dependences reflect the quantitative limitations of this type of calculation.

To clarify more the interpretation of our results, a few MD runs for the KI pair at fixed interionic distances were made for $\rho_1 = 25$ mol·dm^{-3} and 420 K using the same procedure to obtain

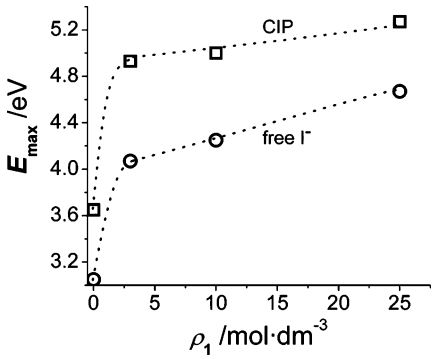

Figure 8. Calculated values of E_{max} for CIP (□) and free I^- (○) as function of solvent density at 420 K. Dotted lines represent the expected behavior.

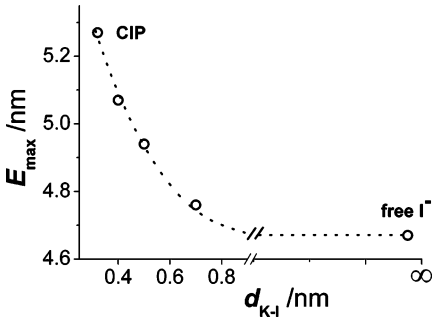

Figure 9. Calculated E_{max} (○) for different values of fixed K^+-I^- distances at 420 K and $\rho_1 = 25$ mol·dm^{-3}.

E_{max}; the results are plotted in Figure 9. It is clear that the energy of the transition in the pair becomes very close to that in the free iodide ion when the interionic distance is greater than 0.7 nm. Hence, we conclude that the spectral behavior of the free I^- and SSIP are the same within the precision of our measurements.

Discussion

Ion pair dissociation is a process that leads to charge separation and is influenced by the dielectric constant of the solvent, a property that is strongly dependent on ρ_1 for supercritical solvents. Hnizda and Kraus[26] measured the electrolytic conductivity of KI solutions in liquid ammonia at 239 K and saturation pressure, and they found that the salt was weakly dissociated and the dissociation equilibrium constant (in the molarity scale) was 4.07×10^{-3}. At that temperature, the experimental dielectric constant of NH_3 is $\epsilon_D = 25$.[8] It is a well-known fact that many electrolyte solutions, at low, reduced temperature, which is inversely proportional to ($\epsilon_D T$), present two types of ion pairs, namely, contact and solvent separated ion pairs; hence, ion pairing equilibria can be represented by a two-step equilibrium. This two-step association has been shown to exist for (2:2) electrolytes in water at high temperatures[27] and also observed by molecular dynamics simulation in univalent aqueous electrolytes at supercritical temperatures.[28] Conductivity measurements give the overall association constant K_A which includes the CIP and SSIP as species that do not contribute to the conductivity of the solution. The K_A value for this two-step equilibrium is given in terms of the association constants for each step by

$$K_A = K_1(1 + K_2) \tag{4}$$

For KI dissolved in tetrahydrofurane (THF), a low-polarity liquid solvent, a change of E_{max} was reported when the alkali metal cation was replaced by a substituted ammonium cation;[7] the difference between the cations Na^+ and Cs^+ was within the experimental uncertainty so it was not observed. In ammonia, we were able to observe clearly the change in E_{max} when the alkali metal cation was changed because, in our solutions at 418 K and ρ_1 below 12 mol·dm^{-3}, the iodides are fundamentally CIPs, while in THF at 298 K, the solvent studied by Blandamer et al.,[7] a significant fraction of ions are SSIPs or free at the low concentrations they employ.

To compare our MD results with the experimental information available for KI solutions in other dense liquids, we chose solvents where the extent of ionic association was expected to be similar to our simulated system, that is, implying similar ($\epsilon_D T$) according to the primitive model which is applicable to high-density SCA. Using the experimental value of the dissociation of KI in pyridine at 298 K,[29] which has $\epsilon_D T = 3700$ a value relatively close to that of NH_3 in our MD simulations at the same temperature ($\epsilon_D T = 2950$), we estimated a value of the dissociation constant of KI in MD−ammonia of 2×10^{-4} at 298 K. Moreover, it should be noted that the concentration of KI in the MD runs is larger than 0.03 mol·dm^{-3}, a value much greater than the experimental concentration. Hence, the fraction of associated species found with the MD calculations should be appreciably larger than that existing under our experimental conditions with concentrations usually below 10^{-4} mol·dm^{-3}. Figures 5 and 6 show that almost no free iodide ion is present within the simulation box, and this is expected due to the differences in the solute concentration and ϵ_D between the MD simulations and the actual experiments that were noted above.

Although the results about speciation obtained from MD are essentially of qualitative nature, it is expected that simulation runs will account properly for the solvent structure around the solute for a given species, namely, CIP or free I^-. This is verified by the agreement between the experimental and calculated E_{max} values for CIPs and I^- as well as their solvent density dependence. In addition, at 418 K the measured spectral FWHM value (0.5 ± 0.1 eV for both CIP and I^- at all ρ_1 values) matched that obtained with the theory (0.52 ± 0.05 eV) for the CIP.

The observation that E_{max} for CIPs is almost unaffected by changes of ρ_1 over a wide range suggests that a well-organized solvent structure is already established around the KI molecule at the lowest densities studied in the present work, and hence, the solvation energy of both ground (K^+-I^-) and excited ($K^+-I + e^-$) states are similarly affected. On the other hand, the E_{max} for the SSIP or free I^- was found to be sensitive to the density of the medium because in this case the transition takes place in a less structured medium and outside the K^+ first solvation shell. It is expected that the excited state of the CIP will appear similar to the ground state of alkali metals M dissolved in NH_3 clusters if one ignores the small contribution the iodine atom has on the energy of the system. The structure of alkali metal atoms in ammonia clusters containing more than 10 NH_3 molecules consists of M^+ and a solvated electron according to experimental data by Hertel et al.[30] Moreover, it should be noted that Martyna and Klein[31] observed that the solvent structure for $M(NH_3)_n$ clusters is very similar to that for $M^+(NH_3)_n$ so that the solvated electron plays a secondary role over solvent structure.

In summary, the combination of the MD and quantum calculation methods used in this work have demonstrated to be adequate for describing the nature of the electronic transition for this kind of system. This approach will be used in a forthcoming article in order to address the following questions: (i) Is it possible to expect an interionic charge transfer,

similar to that in the vapor, when the CIP is solvated by a polar solvent? (ii) How is the usual CTTS transition of free iodide in polar solvents modified by the presence of counterions?

Conclusions

The use of SCA has allowed us to observe for the first time two contributions to the UV-absorption spectrum of dissolved KI due to the existence of different species; their relative weight depends on the fluid density and temperature. At low fluid density and high temperature, the H-band is explained by the presence of contact ion pairs and, as density increases, by either increasing pressure or decreasing temperature. A second contribution, the L-band, becomes progressively more significant, and this was assigned to the electron excitation when the cation and anion are separated by more than 0.7 nm, whether they are free ions or form solvent separated ion pairs. The analysis of the spectrum of KI dissolved in ammonia under liquid−vapor equilibrium over a range of temperatures enabled us to confirm the presence of two absorbing species in the solutions we have studied. It is interesting to remark that as a collateral advantage the spectroscopic results can discriminate between the CIP and other species.

The results of this study show the importance of the presence of the cation to characterize the spectra, especially when KI is forming CIPs. On the other hand, even at low solvent densities when the CIP is the prevalent species in solution, the electronic excitation process is different from that in the vapor phase.

Finally, we conclude that the information provided by the study of clusters that contain only the I^- ion is not easily related to the behavior in bulk solvents when ion pairs exist because no account is taken of the influence of the cation; hence it would only correspond to the excitation observed in strongly polar media where the prevalent species is the free iodide ion.

Acknowledgment. We thank D. Case (UCSF) and M. Marti (UBA) for technical assistance regarding molecular dynamics calculations and Dr. D. Estrín for helpful comments about the ab initio calculations. We are grateful for partial economic support given by ANPCyT (PICT 6818) and UBACyT (X-218). E.M. and R.F.P. are members of the Carrera del Investigador (CONICET, Argentina), and G.S. thanks CONICET (Argentina) for a doctoral fellowship.

References and Notes

(1) Blandamer, M. J.; Fox, M. F. *Chem. Rev.* **1970**, *70*, 59−93.

(2) Crawford, O. H. *Mol. Phys.* **1971**, *20*, 585−591.

(3) Sexner, D.; Dessent, C. E. H.; Johnson, M. A. *J. Chem. Phys.* **1996**, *105*, 7231−7234. Frischkorn, C.; Zanni, M. T.; Davis, A. V.; Neumark, D. M. *Faraday Discuss.* **2000**, *115*, 49−62. Sheu, W.-S.; Rossky, P. J. *J. Chem. Phys.* **1993**, *115*, 7729−7735.

(4) Jouvet, C.; Martrenchard, S.; Solgadi, D.; Dedonder-Lardeux, D.; Mons, M.; Grégoire, G.; Dimicoli, I.; Piuzzi, F.; Visticot, J. P.; Mestdagh, J. M.; D′Oliverida, P.; Meynadier, P.; Perdrix, M. *J. Phys. Chem. A* **1997**, *101*, 2555−2576. Grégoire, G.; Mons, M.; Dedonder-Lardeux, D.; Jouvet, C. *Eur. Phys. J. D* **1998**, *1*, 5−7. Grégoire, G.; Mons, M.; Dimicoli, I.; Dedonder-Lardeux, D.; Jouvet, C.; Martrenchard S.; Solgadi, D. *J Chem. Phys.* **1999**, *110*, 1521−1525.

(5) Smallwood, C. J.; Bosma, W. B.; Larsen, R. E.; Schwartz, B. J. *J. Chem. Phys.* **2003**, *119*, 11263−11277.

(6) Chen, H.-Y.; Shen, W.-S. *J. Am. Chem. Soc.* **2000**, *122*, 7534−7542.

(7) Blandamer, M. J.; Gough, T. E.; Symons, M. C. R. *Trans. Faraday Soc.* **1966**, *62*, 286−295.

(8) Buback, M.; Harder, W. D. *Ber. Bunsen-Ges.* **1977**, *81*, 603−609, 609−614, 735−739.

(9) Sciaini, G.; Marceca, E.; Fernández-Prini, R. *J. Supercrit. Fluids* **2005**, *35*, 106−110.

(10) Tillner-Roth, R.; Harns-Wartzenberg, F.; Bähr, H. D. *Proceedings of the 20th DKV-Tagung*; Heidelberg, Germany, 1993; Vol. II, p 162.

(11) Fernández-Prini, R. *J. Phys. Chem. B* **2002**, *106*, 3217−3225.

(12) Case, D. A.; Darden, T. A.; Cheatham, T. E., III; Simmerling, C. L.; Wang, J.; Duke, R. E.; Luo, R.; Merz, K. M.; Wang, B.; Pearlman, D. A.; Crowley, M.; Brozell, S.; Tsui, V.; Gohlke, H.; Mongan, J.; Hornak, V.; Cui, G.; Beroza, P.; Schafmeister, C.; Caldwell, J. W.; Ross, W. S.; Kollman, P. A. *AMBER8*; University of California: San Francisco, 2004.

(13) Impey, W.; Klein, M. L. *Chem. Phys. Lett.* **1984**, *104*, 579−582.

(14) Evans, D. H.; Keesee, R.G.; Castleman, A. W. *J. Chem. Phys.* **1987**, *86*, 2927−2931.

(15) Mayer, J. E.; Helmholz, T. *Z. Phys.* **1932**, *75*, 19−28.

(16) Hartley, H. G.; Fink, M. *J. Chem. Phys.* **1988**, *89*, 6053−6057.

(17) Kindt, J. T.; Schmuttenmaer, C. A. *J. Chem. Phys.* **1997**, *106*, 4389−4400.

(18) Diraison, M; Martyna, G. J.; Tuckerman, M. E. *J. Chem. Phys.* **1999**, *111*, 1096−1103.

(19) Rodríguez, J.; Skaf, M. S.; Laria, D. H. *J. Chem. Phys.* **2003**, *119*, 8044−8052.

(20) Frisch, M. J.; Trucks, G. W.; Schlegel, H. B.; Scuseria, G. E.; Robb, M. A.; Cheeseman, J. R.; Zakrzewski, V. G.; Montgomery, J. A., Jr.; Stratmann, R. E.; Burant, J. C.; Dapprich, S.; Millam, J. M.; Daniels, A. D.; Kudin, K. N.; Strain, M. C.; Farkas, O.; Tomasi, J.; Barone, V.; Cossi, M.; Cammi, R.; Mennucci, B.; Pomelli, C.; Adamo, C.; Clifford, S.; Ochterski, J.; Petersson, G. A.; Ayala, P. Y.; Cui, Q.; Morokuma, K.; Malick, D. K.; Rabuck, A. D.; Raghavachari, K.; Foresman, J. B.; Cioslowski, J.; Ortiz, J. V.; Stefanov, B. B.; Liu, G.; Liashenko, A.; Piskorz, P.; Komaromi, I.; Gomperts, R.; Martin, R. L.; Fox, D. J.; Keith, T.; Al-Laham, M. A.; Peng, C. Y.; Nanayakkara, A.; Gonzalez, C.; Challacombe, M.; Gill, P. M. W.; Johnson, B. G.; Chen, W.; Wong, M. W.; Andres, J. L.; Head-Gordon, M.; Replogle, E. S.; Pople, J. A. *Gaussian 98*; Gaussian, Inc.: Pittsburgh, PA, 1998.

(21) Bradforth, S. E.; Jungwirth, P. *J. Phys. Chem. A* **2002**, *106*, 1286−1298.

(22) Nelson, J. T.; Cuthrell, R. E.; Lagowski, J. J. *J. Phys. Chem.* **1966**, *70*, 1492−1495.

(23) Shapira, D.; Treinin, A. *J. Phys. Chem.* **1966**, *70*, 305−306.

(24) Hotop, H.; Lineberger, W. C. *J. Phys. Chem. Ref. Data* **1985**, *14*, 731−750.

(25) Davidovits, P.; Brodhead, D. C. *J. Chem. Phys.* **1967**, *46*, 2968−2973.

(26) Hnizda, V. F.; Kraus, C. A. *J. Am. Chem. Soc.* **1949**, *71*, 1565−1575.

(27) Méndez De Leo, L.; Bianchi, H. L.; Fernández-Prini, R. *J. Chem. Thermodyn.* **2005**, *37*, 503−515.

(28) Chialvo A. A.; Simonson, J. M. *J. Chem. Phys.* **2003**, *118*, 7921−7929.

(29) Fernández-Prini R. In *Physical Chemistry of Organic Solvent Systems*; Covington, A. K.; Dickinson, T., Eds; Plenum Press: London, 1973; pp 525−614.

(30) Hertel, I. V.; Hüglin, C.; Nitsch, C.; Schulz, C. P. *Phys. Rev. Lett.* **1991**, *67*, 1767−1770. Brockhaus, P.; Hertel, I. V.; Schulz, C. P. *J. Chem. Phys.* **1999**, *110*, 393−402.

(31) Martyna, G. J.; Klein, M. L. *J. Chem. Phys.* **1992**, *96*, 7662−7071.